

An Impact Ionization Model Including an Explicit Cold Carrier Population

T. Grasser, H. Kosina, C. Heitzinger, and S. Selberherr

Institute for Microelectronics, TU Vienna, Gusshausstr. 27–29,
A-1040 Vienna, Austria, grasser@iue.tuwien.ac.at

ABSTRACT

Conventional macroscopic impact ionization models which use the average carrier energy as main parameter cannot accurately describe the phenomenon in modern miniaturized devices. Here we present a new model which is based on an analytic expression for the distribution function. In particular, the distribution function model accounts explicitly for a hot and a cold carrier population in the drain region of MOS transistors. The parameters are determined by three even moments obtained from a solution of a six moments transport model. Together with a nonparabolic description of the density of states accurate closed form macroscopic impact ionization models can be derived based on familiar microscopic descriptions.

Keywords: impact ionization modeling, moment equations, BOLTZMANN equation, distribution function model.

1 INTRODUCTION

Accurate calculation of impact ionization rates in macroscopic transport models is becoming more and more important due to the ongoing feature size reduction of modern semiconductor devices. Conventional models which use the average carrier energy as main parameter fail because impact ionization is very sensitive to the shape of the distribution function, in particular to the high-energy tail. The average energy is not sufficient for obtaining this information and higher order moments of the distribution function have to be considered. We favor a local description because the scattering operator in Boltzmann's equation is a functional of the local distribution function which should be reflected by the model.

2 PREVIOUS MODEL

Here we present a refined version of a previously published model [1] developed for the use with a six moments transport model [2] which also accounts for the kurtosis of the distribution function,

$$\beta_n = \frac{3 \langle \mathcal{E}^2 \rangle}{5 \langle \mathcal{E} \rangle^2} \quad (1)$$

in addition to the carrier temperature. So far, we have used

$$f(\mathcal{E}) = A \exp \left[- \left(\frac{\mathcal{E}}{\mathcal{E}_{\text{ref}}} \right)^b \right] \quad (2)$$

for the symmetric part of the distribution function and

$$g(\mathcal{E}) = g_0 \sqrt{\mathcal{E}} \left(1 + (\eta \mathcal{E})^\zeta \right) \quad (3)$$

for the nonparabolic density of states, respectively. The parameters $\mathcal{E}_{\text{ref}} = \mathcal{E}_{\text{ref}}(T_n, \beta_n)$ and $b = b(T_n, \beta_n)$ are functions of the carrier temperature and kurtosis and are determined in such a way that $f(\mathcal{E})$ reproduces the given moments T_n and β_n [1]. The parameters η and ζ of (3) are determined by a fit to either Kane's dispersion relation [3] or to pseudo-potential data [1]. Due to the form of the fit expression for the density of states (3) it is possible to give algebraic expressions for the moments of (2) using Gamma functions. With the parameter values $\eta = 1.4 \text{ eV}^{-1}$ and $\zeta = 1.08$ the error in the first three even moments was found to be smaller than 1% when compared to the results obtained from Kane's relation.

Expression (2) is accurate inside the channel of MOS transistors with values of $b > 1$. Although (2) gives reasonable approximations for the distribution function inside the drain region ($b < 1$) there are two problems: Firstly, the high-energy tail is overestimated and secondly, during the transition from the channel to the drain region, the exponent b assumes the value 1 which corresponds to a Maxwellian distribution function, a result not confirmed by Monte Carlo simulations. This error is amplified when for instance impact ionization rates are calculated where only the high-energy tail of the distribution function is required [1].

3 DISTRIBUTION FUNCTION MODEL

To improve the model we note that at the drain junction the hot carriers from the channel meet a large pool of cold carriers and two populations coexist. We account for this fact by using a superposition of two distributions, similar to the work of Sonoda *et al.* [4]

$$f(\mathcal{E}) = A \left\{ \underbrace{\exp \left[- \left(\frac{\mathcal{E}}{\mathcal{E}_{\text{ref}}} \right)^b \right]}_{f_1(\mathcal{E})} + c \underbrace{\exp \left[- \frac{\mathcal{E}}{k_B T_2} \right]}_{f_2(\mathcal{E})} \right\} \quad (4)$$

We now have to determine the five parameters A , \mathcal{E}_{ref} , b , c , and T_2 which describe the distribution function, that is, we need two heuristic relations in addition to the three parameters n , T_n , and β_n provided by the six moments model. To get an idea about the behavior of the distribution function in the drain region we look at the second order moment T_1 and the fourth order moment β_1 of the hot distribution $f_1(\mathcal{E})$ only (Fig. 1) which was extracted from the total distribution function obtained by a Monte Carlo simulation in a post-processing step. The kurtosis of the hot distribution is defined as

$$\beta_1 = \frac{3}{5} \frac{\int f_1 g d\mathcal{E} \int \mathcal{E}^2 f_1 g d\mathcal{E}}{(\int \mathcal{E} f_1 g d\mathcal{E})^2} \quad (5)$$

Additional simulations show that the temperature T_2 of the cold Maxwellian distribution function $f_2(\mathcal{E})$ rapidly relaxes to the lattice temperature T_L and will be modeled as $T_2 = T_L$ in this work. The kurtosis β_1 , however, is crucial for an accurate description of the high-energy tail. Interestingly, β_1 can be modeled accurately via the bulk relation $\beta_{\text{Bulk}}(T_n)$ which can be derived from the homogeneous six moments model [2] as

$$\beta_{\text{Bulk}}(T_n) = \frac{T_L^2}{T_n^2} + 2 \frac{\tau_\beta \mu_S}{\tau_\mathcal{E} \mu_n} \left(1 - \frac{T_L}{T_n}\right) \quad (6)$$

where $\tau_\mathcal{E}$, τ_β , μ_n , and μ_S are the energy relaxation time, the kurtosis relaxation time, the electron mobility, and the energy flux mobility, respectively.

A comparison of the model $\beta_1 = \beta_{\text{Bulk}}(T_1)$ with Monte Carlo data is shown in Fig. 1, where the temperature of the high-energy tail T_1 has been taken as the argument. Note that $\beta_{\text{Bulk}}(T_n)$ approaches unity too quickly which underlines the idea of modeling the hot and cold electrons as separate populations.

For the calculation of the parameters \mathcal{E}_{ref} , b , and c we have to detect the regions where a cold population exists. Monte Carlo simulations show that inside the channel the tail of the distribution function is always less populated than in the bulk case. Therefore we detect the drain region when $\beta_n > \beta_{\text{Bulk}}(T_n)$ is fulfilled. Inside the channel we assume $c = 0$ because no cold subpopulation exists. Inside the drain region, however, we need to determine c and T_2 to explicitly allow for two separate populations.

Thus nonlinear equation system is solved using Newton's method

$$\begin{pmatrix} T_n(\mathcal{E}_{\text{ref}}, b, c) \\ \beta_n(\mathcal{E}_{\text{ref}}, b, c) \\ \beta_1(\mathcal{E}_{\text{ref}}, b, c) \end{pmatrix} = \begin{pmatrix} T_n^{\text{MC}} \\ \beta_n^{\text{MC}} \\ \beta_{\text{Bulk}}(T_1(\mathcal{E}_{\text{ref}}, b, c)) \end{pmatrix} \quad (7)$$

T_n , β_n , and β_1 are analytic expressions derived from the moments of (4) and T_n^{MC} and β_n^{MC} were taken from Monte

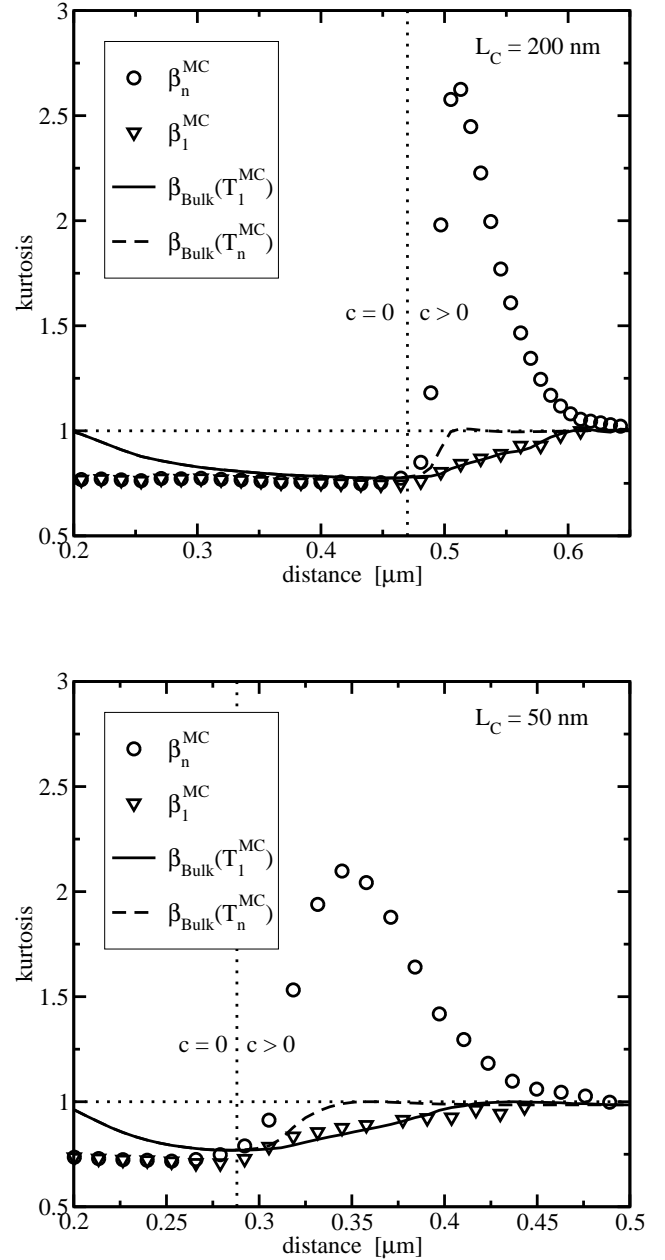


Figure 1: Comparison of β_1^{MC} with two analytical models. When the temperature of the hot distribution function T_1 is used in the bulk characteristic, accurate results are obtained for n^+-n-n^+ test-structures with $L_C = 200$ nm and $L_C = 50$ nm. Note that $\beta_{\text{Bulk}}(T_n)$ does not properly describe the behavior of β_1 . Also shown is the kurtosis of the total distribution function β_n .

Carlo simulations. In the channel $c = 0$ is assumed and the last row of (7) is dropped. Since there is no cold population $T_1 = T_n$ holds inside the channel. This also holds at the transition point which guarantees a continuous transition between the two regions. A comparison with distribution

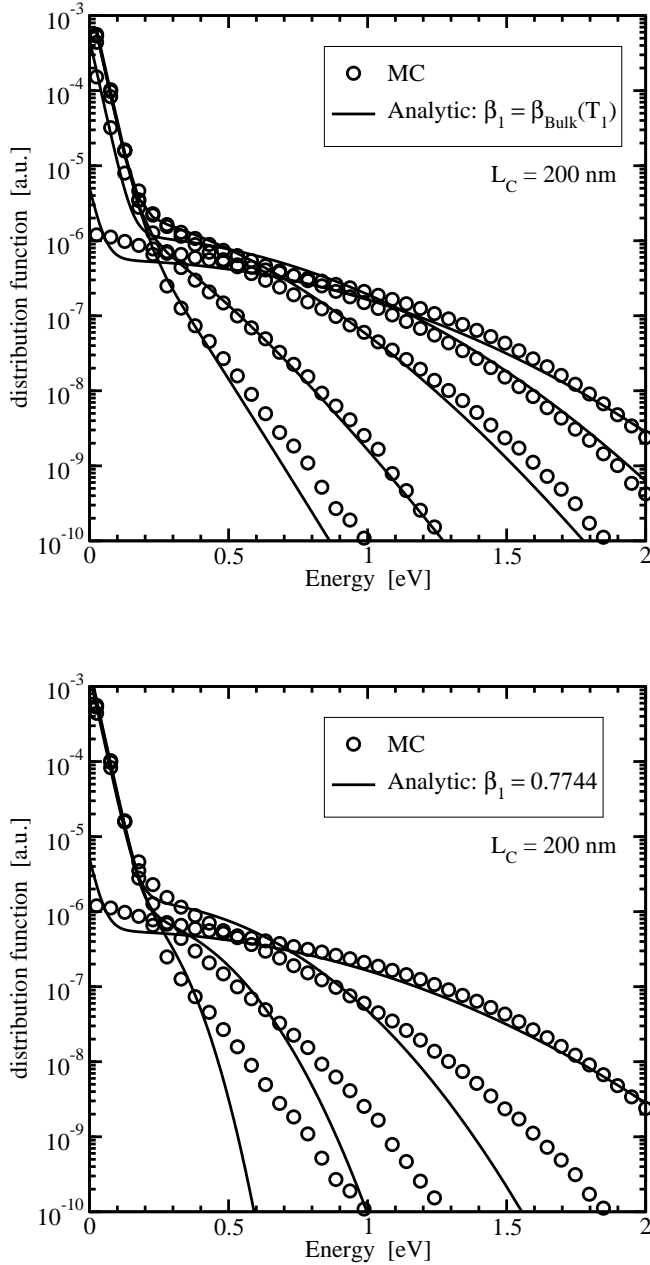


Figure 2: Comparison of analytical expressions for the distribution function with Monte Carlo results at different positions inside an $n^+ - n - n^+$ test-structure with $L_C = 200$ nm. Note the error in the tail when a constant value for β_1 is assumed (bottom figure).

functions obtained by Monte Carlo simulations is shown in Fig. 2. Note that a constant value for $\beta_1 = \beta_h$ as used in [4] underestimates the tail of the distribution function and thus the associated impact ionization rate. Furthermore, an approach based on a constant β_1 works only for the high field case because otherwise β_n will never reach β_h and the model erroneously creates a cold population throughout the whole

device. For intermediate bias conditions a spurious cold population would be predicted in the larger part of channel.

4 IMPACT IONIZATION MODEL

A closed form macroscopic impact ionization rate is then obtained by integrating Keldysh's expression [5]

$$P_{II}(\mathcal{E}) = P_0 \left(\frac{\mathcal{E} - \mathcal{E}_{th}}{\mathcal{E}_{th}} \right)^2 \quad (8)$$

with (2) and (3) as

$$G_{II,l} = \int_{\mathcal{E}_{th}}^{\infty} \mathcal{E}^l P_{II}(\mathcal{E}) f(\mathcal{E}) g(\mathcal{E}) d\mathcal{E} \quad (9)$$

$$\approx \int_{\mathcal{E}_{th}}^{\infty} \mathcal{E}^l P_{II}(\mathcal{E}) f_1(\mathcal{E}) g_c(\mathcal{E}) d\mathcal{E} \quad (10)$$

$$= n P_0 \mathcal{E}_{ref}^l \left(\frac{\mathcal{E}_{ref}}{\mathcal{E}_C} \right)^{\lambda-1/2} \times \frac{\Gamma_{1,l} - 2z_{th}^{-1/b} \Gamma_{2,l} + z_{th}^{-2/b} \Gamma_{3,l}}{\Gamma\left(\frac{2l+3}{2b}\right) + (\eta \mathcal{E}_{ref})^\zeta \Gamma\left(\frac{2l+2\zeta+3}{2b}\right)} \quad (11)$$

where $\Gamma(a, z)$ is the incomplete Gamma function and

$$\Gamma_{j,l} = \Gamma\left(\frac{j+l+\lambda}{b}, z_{th}\right) \quad (12)$$

$$z_{th} = \left(\frac{\mathcal{E}_{th}}{\mathcal{E}_{ref}}\right)^b \quad (13)$$

$$g_c(\mathcal{E}) = g_0 \sqrt{\mathcal{E}_C} \left(\frac{\mathcal{E}}{\mathcal{E}_C}\right)^\lambda \quad (14)$$

Equation (14) is an approximation of the high-energy region of the density of states ($\mathcal{E}_C = 0.35$ eV and $\lambda = 1.326$), based on Cassi and Riccò's [6] model, which has been introduced to simplify the final expression. Furthermore, it is assumed that only $f_1(\mathcal{E})$ contributes to the impact ionization rate. In (11) $l = 0, 1, 2$ and denotes the entries for the continuity, energy balance, and kurtosis balance equations, respectively.

5 COMPARISON

The final expression (11) is equivalent to the expression given in [1], but the parameters \mathcal{E}_{ref} and b are now calculated in a different way. We use the same parameter values as in the Monte Carlo simulation ($P_0 = 4.18 \times 10^{12} \text{ s}^{-1}$, $\mathcal{E}_{th} = 1.12$ eV), values which fit available experimental data for bulk. The accuracy for the bulk case is the same as in [1] as there is no cold population ($c = 0$). A comparison with Monte Carlo simulations for $n^+ - n - n^+$ test-structures is shown in Fig. 3 where the improvement to the model of [1] is obvious. In addition, the results obtained by assuming a

constant β_1 and the results obtained by a Maxwellian distribution function ($\mathcal{E}_{\text{ref}} = k_B T_n$, $b = 1$, and $c = 0$) are shown which underline the importance of an accurate distribution function model for impact ionization rate modeling.

6 CONCLUSIONS

The new macroscopic impact ionization model has been proven to deliver accurate results for the homogenous case [1] and inhomogeneous cases down to nanoscale devices. In particular, the tail of the impact ionization rate inside the drain area is correctly predicted which is not possible with models based on the average carrier energy only. The additional accuracy is provided by the kurtosis of the distribution function which can be obtained via a six moments transport model, that is, a model which is one order higher than conventional energy-transport models. It is important to point out that the same parameters as in the Monte Carlo simulation were used to evaluate the model, so no fitting has been performed. Although we have taken a rather simple expression for the microscopic scattering rate which is known to be not very accurate for energies close to the threshold energy, an extension to more accurate models is straightforward. As the model involves only state variables of the equation system it is well suited for the implementation into conventional numerical device simulators.

ACKNOWLEDGMENT

This work has been partly supported by the *Christian Doppler Forschungsgesellschaft*, Vienna, Austria. Furthermore, the fruitful discussions with Dr. K. Sonoda, Mitsubishi Corp., are gratefully acknowledged.

REFERENCES

- [1] T. Grasser, H. Kosina, and S. Selberherr, "Influence of the Distribution Function Shape and the Band Structure on Impact Ionization Modeling," *J.Appl.Phys.*, vol. 90, no. 12, pp. 6165–6171, 2001.
- [2] T. Grasser, H. Kosina, M. Gritsch, and S. Selberherr, "Using Six Moments of Boltzmann's Transport Equation for Device Simulation," *J.Appl.Phys.*, vol. 90, no. 5, pp. 2389–2396, 2001.
- [3] E.O. Kane, "Band Structure of Indium Antimonide," *J.Phys.Chem.Solids*, vol. 1, pp. 249–261, 1957.
- [4] K. Sonoda, S.T. Dunham, M. Yamaji, K. Taniguchi, and C. Hamaguchi, "Impact Ionization Model Using Average Energy and Average Square Energy of Distribution Function," *Jap.J.Appl.Phys.*, vol. 35, no. 2B, pp. 818–825, 1996.

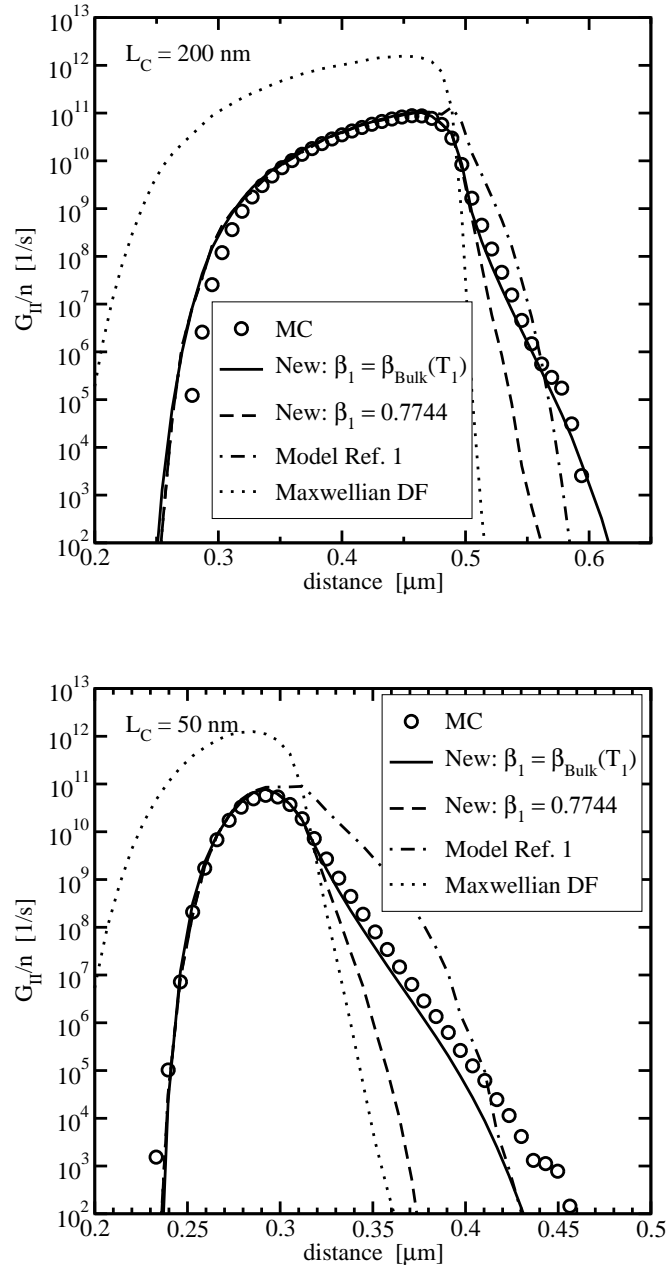


Figure 3: Comparison of analytically obtained impact ionization rates with Monte Carlo results for two $n^+ - n - n^+$ test-structures. Note the improvement to the model of Ref. 1 and the large error when a Maxwellian distribution function is assumed ($E_{\text{max}} = 300 \text{ kV/cm}$).

- [5] L.V. Keldysh, "Concerning the theory of impact ionization in semiconductors," *Sov.Phys.JETP*, vol. 21, pp. 1135–1144, 1965.
- [6] D. Cassi and B. Riccò, "An Analytical Model of the Energy Distribution of Hot Electrons," *IEEE Trans.Electron Devices*, vol. 37, no. 6, pp. 1514–1521, 1990.